Available online at www.sciencedirect.com
SCIENCE DIRECT®
Journal of Nuclear Materials 348 (2006) 302–310
journal of nuclear materials
www.elsevier.com/locate/jnucmat

Tracer diffusion of ^{54}Mn in alloy D9 in presence of sodium

R. Sudha, P. Muralidaran, G. Periaswami, V. Ganesan *

Materials Chemistry Division, Indira Gandhi Centre for Atomic Research, Kalpakkam 603 102, India

Received 28 February 2005; accepted 30 September 2005

Abstract

The diffusivity of manganese in vacuum annealed and cold worked alloy D9 in presence of sodium was measured by the standard tracer technique. The lattice diffusion coefficient of manganese in vacuum annealed alloy D9 specimens in the temperature range 773–873 K is given by the expression $D = (2.24^{+26.45}_{-2.07}) \times 10^{-14} \exp(-60\,764 \pm 17\,403/RT)$ m^2 s^{-1} and that in cold worked alloy D9 specimens is given by $D = (4.62^{+20.77}_{-3.77}) \times 10^{-16} \exp(-38\,880 \pm 12\,006/RT)$ m^2 s^{-1} where R is in J K^{-1} mol^{-1}. The activation energy for diffusion in cold worked specimens is less than that in vacuum annealed specimens. The activation energy for diffusion of manganese in presence of sodium is almost four times less than that in various austenitic stainless steels reported in the literature.
© 2005 Elsevier B.V. All rights reserved.

1. Introduction

The sources of radioactive contamination of the primary circuit of a Sodium Cooled Fast Reactor include activated corrosion products from the structural and clad materials as well as fission products from defective fuel pins. The major source of contamination in the absence of fuel pin failure is the activated corrosion products. The levels of contamination due to them on out-of-core components that require maintenance are correspondingly high. The important radioactive corrosion products are ^{51}Cr, ^{54}Mn, ^{59}Fe, ^{58}Co, ^{60}Co, ^{65}Zn and ^{182}Ta [1]. Among these, ^{54}Mn is of major concern from the point of view of activity burden on the operating personnel. This nuclide is produced by (n, p) reaction of ^{54}Fe present in the clad and structural materials and has a fairly long half-life of 312 d with γ-energy of 835 keV [2]. Its behaviour in sodium systems is quite different from that of other activated corrosion products. The deposition rate of ^{54}Mn is not as fast as that of other nuclides and only an insignificant downstream effect has been reported [3]. Deposition is significant in areas of high turbulence such as valves and pumps [4] and is not a simple physical adsorption. A thorough knowledge of the release, transport and deposition of this nuclide is essential to understand and model its behaviour in fast reactor coolant circuits. One of the important input parameters for modelling the above process is the diffusion coefficient of ^{54}Mn in structural materials. At the operating temperatures, in addition to transport and deposition to various parts, this radionuclide penetrates into the structural material by diffusion. This leads to complex and costly operation and maintenance procedures. In addition, the

* Corresponding author. Tel.: +91 4114 280098; fax: +91 4114 280065.
E-mail address: ganesh@igcar.ernet.in (V. Ganesan).

0022-3115/$ - see front matter © 2005 Elsevier B.V. All rights reserved.
doi:10.1016/j.jnucmat.2005.09.021

diffusion of radionuclides into the structural material renders component decontamination procedures difficult and inadequate. Hence knowledge of the diffusion coefficient of manganese in alloy D9, which is the candidate-clad material in Prototype Fast Breeder Reactor, becomes important. This paper describes the application of tracer technique in determining the diffusion coefficient of ^{54}Mn in alloy D9 in presence of sodium.

2. Tracer technique – residual radioactivity method

The use of high specific activity radiotracers helps in experimental investigation of the fundamental mechanism of atomic diffusion in crystalline solids. The diffusion of the impurity atom can be studied at infinite dilution wherein the solute–solute interactions can be neglected. Also radiotracer techniques are easier to carry out at extremely low concentrations than in chemical analysis and provide accurate data on concentration profiles. In the 'classical' radiotracer technique, radioactive isotopes of the element whose diffusion needs to be investigated are deposited on the specimen surface either by electroplating, vapour deposition or by decomposition of an inorganic salt prior to diffusion annealing. In the present study, the radioisotope of interest, namely ^{54}Mn, was taken in sodium. Owing to this, during diffusion annealing, the concentration of ^{54}Mn on the specimen surface remained constant throughout. The specimen was then diffusion-annealed in a furnace at temperature T at which the diffusion coefficient is to be measured. The duration 't' of annealing needs to be chosen such that it does not exceed the half-life of the isotope while the penetration depth of the radiotracer atoms is distinctly larger than the average thickness of the layers to be removed from the specimen after diffusion annealing. Generally, thin layers are removed from the specimen surface either by sputtering techniques, anodic oxidation, chemical stripping, ultra microtomes, chemical dissolution or electropolishing.

In the present study microsectioning was done by electropolishing. The residual radioactivity on the specimen was measured and the concentration profile was obtained by plotting logarithm of activity vs. the square of the distance from the surface. This profile was fitted against a standard solution of Fick's second law and the diffusion coefficient at the given temperature was determined. The experiment was repeated for several other temperatures. From the Arrhenius representation of the diffusion coefficient, the diffusion parameters, pre-exponential factor D_0 and activation energy E_a were obtained.

3. Experimental

Liquid sodium containing known activity of ^{54}Mn was taken in an alumina crucible. Rectangular sheet specimens of alloy D9 ($20 \times 10 \times 1.2$ mm) were kept immersed in liquid sodium taken in the alumina crucible. In this work vacuum annealed (VA) and cold worked (CW) specimens, whose chemical composition in weight percentage is given in Table 1, were used for diffusion experiments. The crucible along with its contents was placed inside a stainless steel reaction vessel and was secured leak tight using knife-edged flanges employing annealed copper ring as gasket material. The entire operation was carried out in a high purity argon atmosphere glove box. The specimens were then diffusion annealed at temperatures ranging from 773 to 873 K for different periods of time from 1.8×10^6 to 10.8×10^6 s. At the end of diffusion annealing, the specimens were cleaned free of sodium, dried, weighed and the residual activity of ^{54}Mn was measured using a well-type NaI (Tl) detector after microsectioning of the layers electrochemically. A mixture of 65% phosphoric acid, 20% sulphuric acid and 15% distilled water by volume was used as electrolyte and a current density of 0.2 A cm^{-2} was employed. Electropolishing for 60 s removed approximately 1 μm of the material. Concentration profiles of ^{54}Mn were obtained by plotting the residual radioactivity on the specimens measured after each electropolishing step as a function of square of distance from the initial specimen surface. The thickness of the layers removed was determined using weight loss method. The temperature dependence of D was calculated by plotting $\log D$ vs. $1/T$. From this plot, the Arrhenius parameters D_0 and E_a were determined.

Table 1
Chemical composition of alloy D9 in wt%

C	Si	Mn	Ni	Cr	Mo	S	P	Co	Ti	Ta + Nb	N	B	Fe
0.052	0.505	1.509	15.068	15.051	2.248	0.003	0.011	0.0515	0.315	0.020	0.007	0.001	Bal

4. Results and discussion

From the free energies of formation of metal chlorides, it is known [5] that manganese chloride gets reduced to manganese in sodium. During diffusion annealing, the radioisotope dissolved in sodium maintains a constant concentration at the surface of the specimen, some of which penetrates the specimen surface by diffusion. Since the diffusion length of the radioisotope is extremely small in comparison with the thickness of the specimen, the concentration of ^{54}Mn on the sample surface is assumed to be constant considering the bulk ^{54}Mn activity in sodium. Hence, the solution of Fick's second law of diffusion as applied to semi-infinite body is applied in the present case. The residual activity is related to the thickness of the layer removed by the following expression [6]:

$$\ln A = \ln \frac{C_0}{2\sqrt{\pi D t}} - \frac{x^2}{4Dt}, \quad (1)$$

where A = residual activity (Bq), C_0 = constant concentration of ^{54}Mn on the specimen surface (Bq), D = diffusion coefficient ($m^2\ s^{-1}$), t = diffusion annealing time (s) and x = diffusion length (m).

The penetration plot is obtained by plotting the logarithm of the residual radioactivity against the square of the diffusion length. Figs. 1 and 2 show the penetration plots in vacuum annealed and cold worked specimens. These plots have three linear regions with different slopes. For elucidating the three regions, a typical concentration profile of vacuum annealed specimen (873 K, 1000 h) is shown in Fig. 3 where the zones are marked. The three zones indicate that the diffusion of the deposited radioisotope in the structural material takes place by three distinct processes. The outermost zone (zone 1 in Fig. 3) corresponds to the manganese radioactivity in the depleted layer formed by the preferential dissolution of Ni and Cr from the specimen into sodium. Hence over a period of time the austenitic surface gets depleted of chromium and nickel. The thickness of the depleted layer varies according to the time and temperature of exposure to sodium and in the present study is of the order of 3–5 μm. Calculation of diffusion coefficient in this region is not considered since this region does not pertain to any phase of interest. The intermediate zone (zone 2) is the zone of interest from where the bulk diffusion in the material is calculated. The diffusion coefficient of the radioisotope in the specimen is determined from the relation, $D = -1/(4\theta t)$, where θ is the gradient of this intermediate zone (refer Eq. (1)). The thickness of the diffusion zone in the present study is found to be in the range of 12–15 μm. Following the intermediate zone, is the diffusion in the tail zone (zone 3). The radioactivity in the tail zone was too less to be counted and corresponds to the background radioactivity with slight contribution from grain boundary diffusion.

In Fig. 1, the data for the penetration plots at temperatures 773 and 798 K appear to exhibit slight scatter. This is explained as follows. Diffusion annealing at lower temperatures require relatively

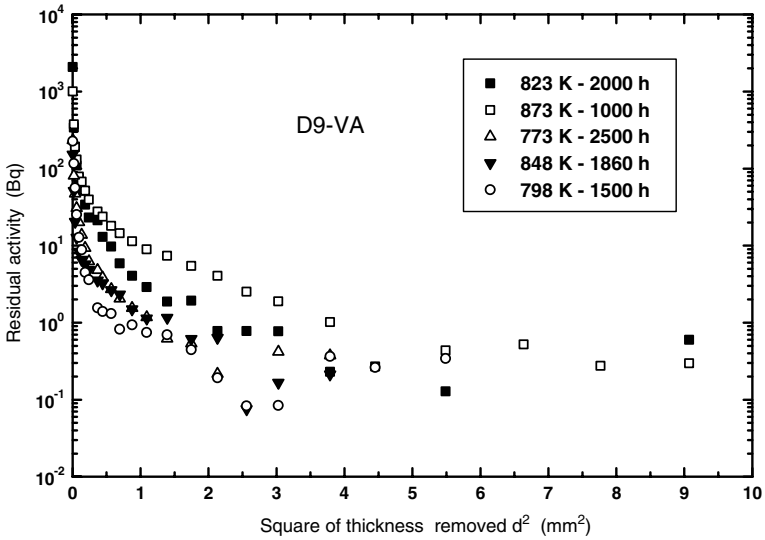

Fig. 1. Residual activity of ^{54}Mn as a function of x^2 in VA specimens.

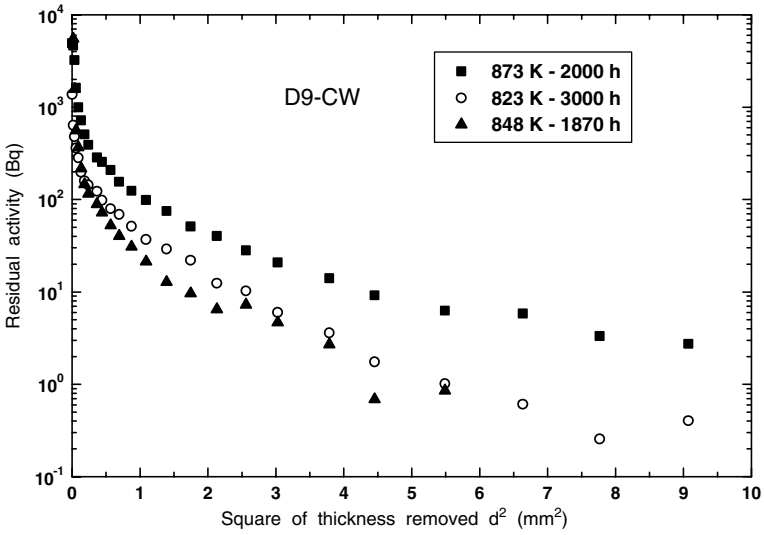

Fig. 2. Residual activity of ^{54}Mn as a function of x^2 in CW specimens.

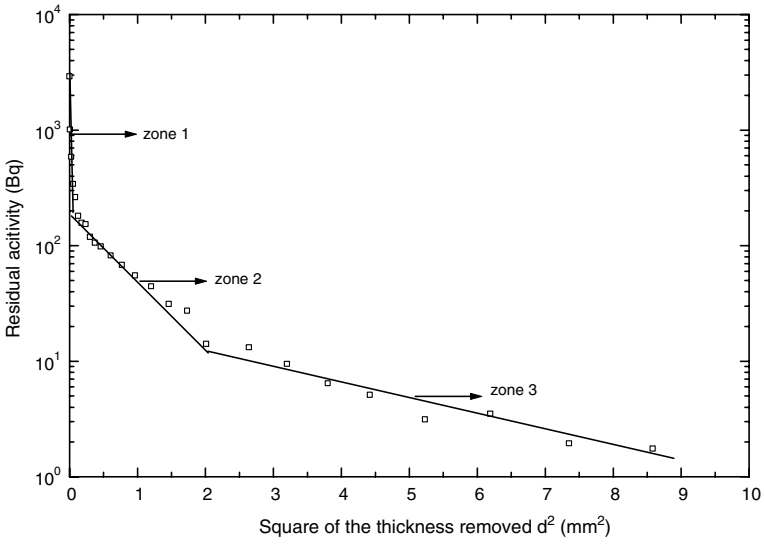

Fig. 3. Typical penetration plot of VA alloy D9 specimen diffusion annealed at 873 K for 1000 h.

higher initial radioactivity and also longer duration of diffusion annealing, as the kinetics of diffusion and the penetration depths are less when compared to diffusion at high temperatures. Hence the radioactive counts were less as measured in the intermediate region at these temperatures. In addition, considering the safety aspects of radioactive handling, high amounts of initial radioactivity was not recommended. It is also well known that the bulk diffusion is a combination of volume diffusion and grain boundary diffusion. At low temperatures the contribution from grain boundaries dominate and at high temperatures the diffusion is mainly due to bulk of the grains. In the present study, the scatter in the data in the intermediate zone at 773 and 798 K is due to low initial radioactivity and relatively short duration of diffusion annealing. However, in all the cases, the intermediate zone (zone 2) was carefully chosen while determining the slopes and calculating the diffusion coefficients.

The microstructures of alloy D9 (both CW and VA), at the start and after diffusion annealing followed by electropolishing, were recorded. The surface of the 20% CW and VA alloy D9 specimens

were examined metallographically before diffusion annealing but the same could not be examined immediately after diffusion annealing as it involves handling high radioactivity inside the SEM chamber. However, the specimens were examined after diffusion annealing followed by electropolishing, which contained radioactivity corresponding to background level. Figs. 4(a) and 4(b) show the microstructures of the 20% CW alloy D9 specimen before diffusion annealing and after diffusion annealing at 873 K for 2000 h followed by electropolishing. In the 20% CW specimen, the slip bands and twin boundaries are clearly seen which is typical in any cold worked specimen, whereas after diffusion annealing, the slip bands and twin boundaries have disappeared. However, there is no significant grain growth during diffusion annealing when compared with the parent 20% CW specimen.

Figs. 5(a) and 5(b) show the microstructure of VA specimen before diffusion annealing and after

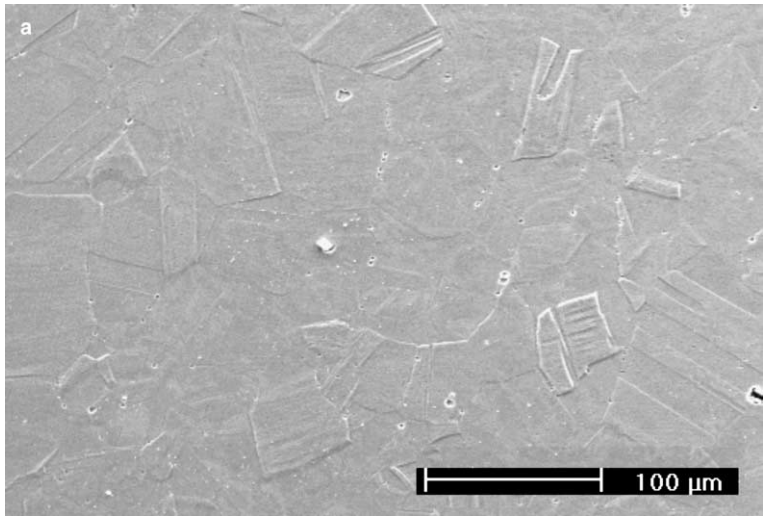

Fig. 4(a). Microstructure of as received 20% CW alloy D9. Slip bands and twin boundaries, typical of cold working, are clearly seen.

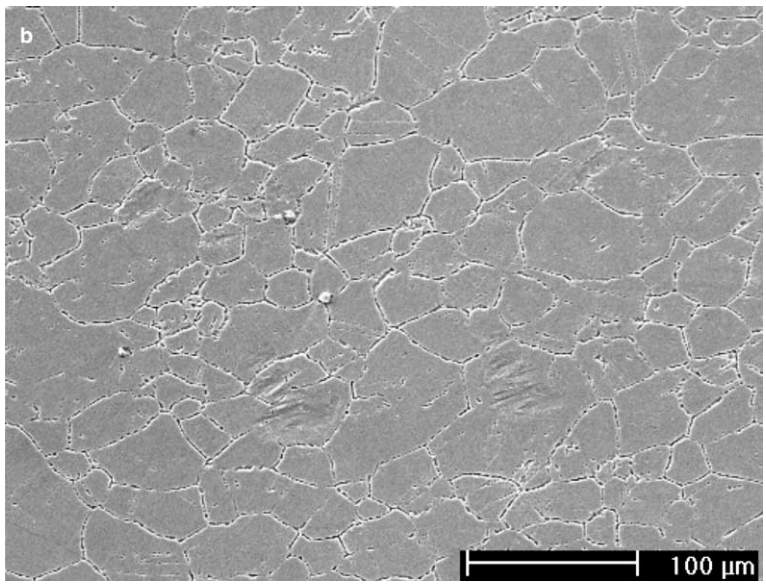

Fig. 4(b). Microstructure of 20% CW alloy D9 after diffusion annealing at 873 K for 2000 h followed by electropolishing. Possible TiC precipitation along the grain boundaries is seen feebly since such processes are postponed by cold working.

diffusion annealing at 873 K for 1000 h followed by electropolishing. D9 is a titanium-modified alloy to avoid chromium carbide precipitation and hence sensitisation at high temperature operation. In Fig. 5(b), possible TiC precipitation along the grain boundaries was prominently observed compared to very slight precipitation seen in the CW specimen since such processes are generally postponed in cold worked materials.

The average grain size of the vacuum annealed specimen as determined by intercept method is 80 μm. However, due to the presence of slip bands and twin boundaries in 20% CW specimen, accurate determination of grain size by intercept method was

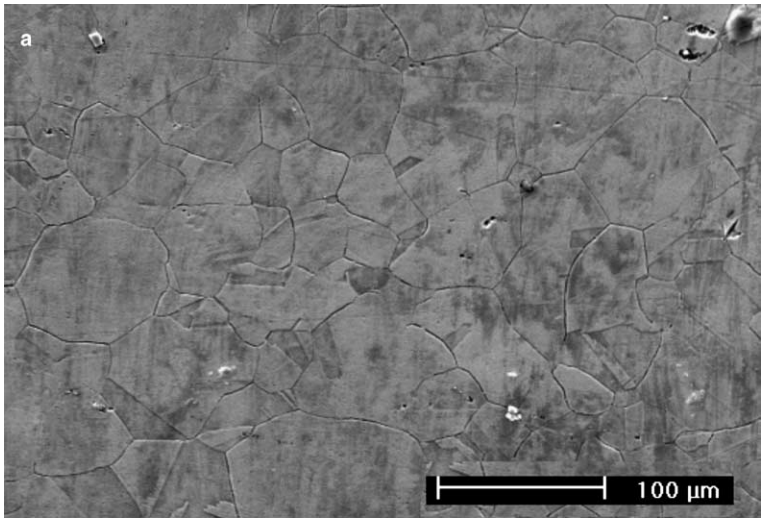

Fig. 5(a). Microstructure of VA alloy D9.

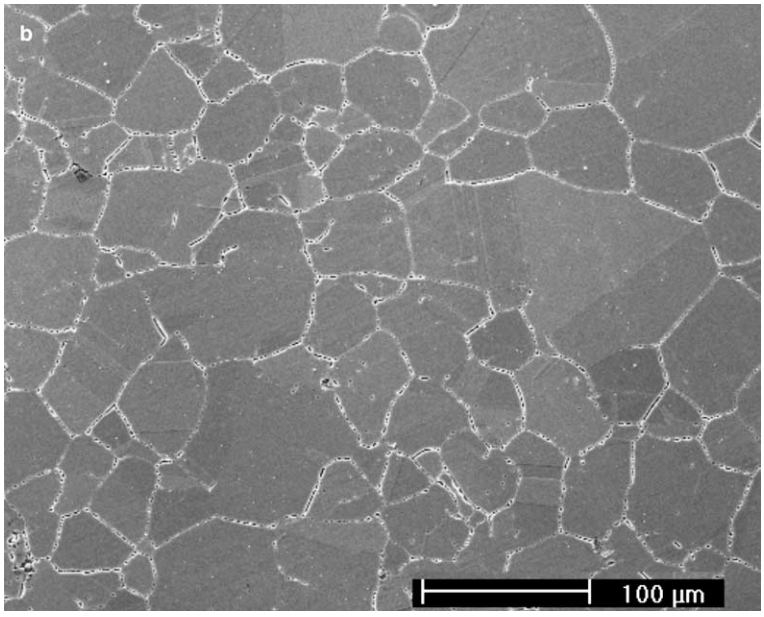

Fig. 5(b). Microstructure of VA alloy D9 after diffusion annealing at 873 K for 1000 h followed by electropolishing. Possible TiC precipitation along the grain boundaries is seen.

difficult. Hence the grain size was calculated for the cold worked specimen after diffusion annealing in sodium at 873 K for 2000 h followed by electropolishing, which revealed the grain boundaries clearly. The average grain size in this specimen was found to be 57 μm.

The values of diffusion coefficient in the present study ranges from 1.99×10^{-18} to 5.79×10^{-18} $m^2 s^{-1}$ for vacuum annealed alloy D9 specimens in the temperature range of 773–873 K and 1.53×10^{-18} to 2.12×10^{-18} $m^2 s^{-1}$ for cold worked alloy D9 specimens in the temperature range of 823–873 K. Fig. 6 shows the dependence of D with $1/T$. The activation energies for diffusion in vacuum annealed and cold worked specimens are calculated to be 60.76 ± 17.40 and 38.88 ± 12.01 kJ mol^{-1}, respectively and the respective frequency factors are $(2.24^{+26.45}_{-2.07}) \times 10^{-14}$ and $(4.62^{+20.77}_{-3.77}) \times 10^{-16}$ $m^2 s^{-1}$. It is known that diffusion in vacuum annealed material is primarily volume diffusion controlled while that in cold worked material is predominantly grain boundary assisted. The decrease in the D_0 value (4.62×10^{-16} $m^2 s^{-1}$) indicates the defect-aided diffusion in the cold worked specimens [7]. The decrease in the activation energy for diffusion as well as the decrease in D_0 value for the cold worked specimen correlate well. It is observed that the diffusion of the radioisotope in cold worked specimens at lower temperatures, namely at 773 and 798 K, is only in the range of 3–5 μm from the surface of the metal and hence the diffusivity could not be calculated at these temperatures even after 10.8×10^6 s of diffusion annealing.

Data on the diffusion of ^{54}Mn in different stainless steel matrices in presence of sodium is not exhaustive [8–11]. The diffusion coefficient values 1.8×10^{-18} $m^2 s^{-1}$ at 856 K and 1×10^{-19} $m^2 s^{-1}$ at 866 K reported by Sagawa et al. [8] and Brehm et al. [9], respectively are different in order. Ortega and Ariza [10] concluded that the diffusivity of ^{54}Mn in stainless steel AISI type 304 in argon atmosphere is greater than that in presence of sodium in the temperature range of 673–1073 K. Similar behaviour was also observed in our experiments. This behaviour is attributed to the following reason. In presence of sodium, owing to the solubility of manganese in sodium, there is an opposing force that restricts its diffusion into the stainless steel matrix while in argon atmosphere no such force for diffusion into the matrix exists. Hence the diffusivity of radioactive manganese in sodium is found to be less than that in argon atmosphere. If the D values of manganese determined in the presence of sodium are compared with those determined by Ortega and Ariza it is found that D at 923 K determined by Ortega is less than that in the present work. This is because the matrix in their study was initially exposed to argon gas for 168 h and

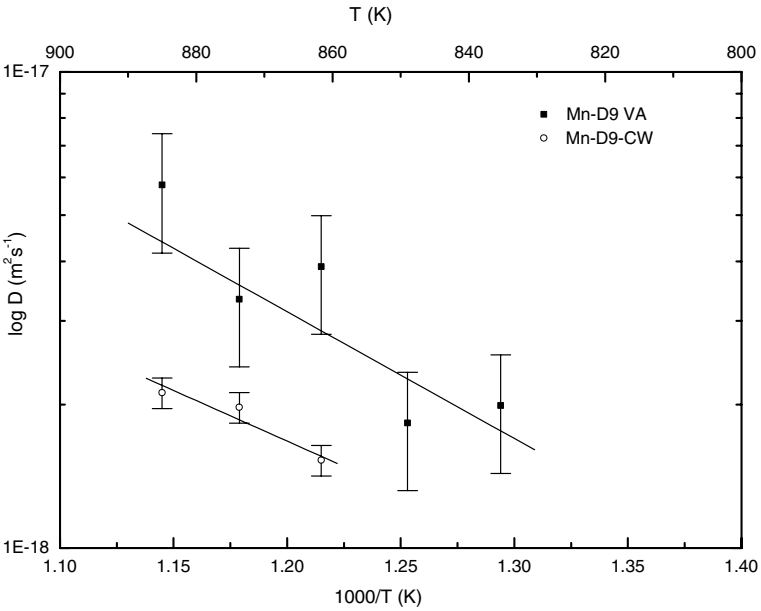

Fig. 6. Bulk diffusion of ^{54}Mn in alloy D9.

then in liquid sodium for another 168 h. Hence the concentration of manganese on the surface would not be a constant and would be depleting as a function of time, whereas in the present work the initial concentration remains constant throughout. The diffusion of ^{54}Mn in AISI type 304 SS was studied earlier [12] by the same technique as in the present work. The D values range from 8.39×10^{-19} to 2.12×10^{-17} m^2 s^{-1} in the temperature range 723–923 K and E_a was found to be 89.51 kJ mol^{-1}. Some of the reports [13–15] discuss about the deposition of ^{54}Mn in the primary circuits of various Fast Reactors while the other reports [16–20] deal with diffusion of ^{54}Mn in austenitic stainless steel and Fe–Mn alloys in the absence of sodium under different experimental conditions. In the present work, the experiment is carried out in presence of sodium. The large difference in the D value reported in the present study compared to those reported earlier is due to the different environment in which the experiments were carried out. It is also interesting to note that the E_a values determined in our experiments are almost four times less than the values reported in literature as shown in Table 2. In the present study, there is a constant surface concentration of ^{54}Mn maintained on the surface of the specimen all through the process. This is responsible for the enhanced diffusion and the low activation energy than that reported in the literature. It is also observed that the E_a for cold worked specimens is less than that for vacuum annealed specimens. This is because in cold worked materials the diffusion is enhanced by dislocations and grain boundaries. From the literature, it is found that diffusion of manganese at high temperatures could be along the grain boundaries into the bulk material while at lower temperatures it remains as Mn–Ni rich phase at the surface [21]. It is well known that longer exposure of the matrix to sodium containing ^{54}Mn at higher temperature results in higher diffusion length. This has direct bearing on decontamination of radioactive components, as it is required to remove only a few μm thickness of the bulk material at low temperatures while at high temperatures several μm thick layers need to be removed.

5. Conclusion

The diffusion coefficient of ^{54}Mn in vacuum annealed alloy D9 in liquid sodium environment measured in the temperature range of 773–873 K was found to vary from 1.99×10^{-18} to $5.79 \times$

Table 2
Comparison of D values with literature data

Diffusing matrix	Temperature (K)	D (m^2 s^{-1})	D_0 (m^2 s^{-1})	E_a (kJ mol^{-1})	Investigator	Experimental technique	Year
SS 304[a]	855	1.8×10^{-17}	–	–	Sagawa et al. [8]	Tracer technique, residual activity	1975
SS 304[a] (VA)	723–923	8.4×10^{-19}–2.1×10^{-17}	2.47×10^{-12}	89.54	Earlier work [12]	Tracer technique, residual activity	1991
SS 316 (VA)	1023–1473	2.18×10^{-18}–2.48×10^{-14}	4.12×10^{-5}	260	Smith and Hales [17]	Tracer technique, residual activity	1975
D9 alloy[a] (VA)	773–873	1.9×10^{-18}–5.79×10^{-18}	2.24×10^{-14}	60.76	Present work	Tracer technique, residual activity	1999
D9 alloy[a] (CW)	823–873	1.53×10^{-18}–2.12×10^{-18}	4.62×10^{-16}	38.88			
Fe–20Cr–25Ni/Nb (VA)	1023–1573	4.83×10^{-18}–1.26×10^{-13}	2.1×10^{-5}	247.5	A.F. Smith [18]	Tracer technique, residual activity	1975
Fe–34%Mn (VA)	1263–1413	7.15×10^{-16}–8.26×10^{-15}	7.3×10^{-6}	242	Nohara and Hirano [20]	Tracer technique, residual activity	1973
Fe–2.97%Mn (VA)	1263–1413	6.32×10^{-16}–5.96×10^{-15}	9.6×10^{-7}	222	Nohara and Hirano [16]	Tracer technique, residual activity	1970
Fe–1.04%Mn (VA)	1263–1413	2.77×10^{-16}–3.43×10^{-15}	5.5×10^{-6}	249	Nohara and Hirano [16]	Tracer technique, residual activity	1970
Pure γ iron (VA)	1263–1413	2.56×10^{-16}–3.59×10^{-15}	1.6×10^{-5}	261	Nohara and Hirano [16]	Tracer technique, residual activity	1970
SS 316[a]	866	1×10^{-19}	–	–	Brehm et al. [9]	Residual activity	1970
SS 304[b]	673–1073	1.685×10^{-19} at 923 K[c]	–	–	Ortega and Ariza [10]	Vac. Sublimation, glow discharge	1984

[a] Diffusion in the presence of sodium.
[b] Specimen exposed initially in Ar gas for 168 h and then in Na for another 168 h.
[c] Values determined from penetration plot.

10^{-18} m^2 s^{-1} and that in cold worked D9 specimens from 1.53×10^{-18} to 2.12×10^{-18} m^2 s^{-1}. Arrhenius parameters D_0 and E_a values were $(2.24^{+26.45}_{-2.07}) \times 10^{-14}$ m^2 s^{-1} and 60.76 ± 17.40 kJ mol^{-1} for vacuum annealed specimens and $(4.62^{+20.77}_{-3.77}) \times 10^{-16}$ m^2 s^{-1} and 38.88 ± 12.01 kJ mol^{-1} for cold worked specimens respectively. The results of the present study show, under the operational conditions of fast reactor, penetration of ^{54}Mn into the stainless steel matrix depends on the thermo-mechanical treatment and operation history of the material.

Acknowledgement

The authors wish to acknowledge the comments and useful suggestions by Dr. Vaidehi Ganesan during the preparation of the manuscript.

References

[1] H. Fuerstein, A.J. Hooper, F.A. Johnson, At. Energy Rev. 173 (1979) 697.
[2] Chart of the Nuclides, Knolls Atomic Power Laboratory, Navel Reactors, US DOE, 15th edition, (1996).
[3] N. Sekiguchi, K. Iizawa, H. Atsumo, IAEA Report IWGFR/7, 1975, p. 82.
[4] K.T. Claxton, J.G. Collier, J. Br. Nucl. Energy Soc. 12 (1973) 63.
[5] D.R. Stull, H. Prophet, JANAF Thermochemical Tables, 2nd ed. NSRDS, NBS-37, USA, 1970.
[6] P.G. Shewmon, Diffusion in Solids, McGraw-Hill, New York, 1989.
[7] J.R. Manning, Diffusion Kinetics for Atoms in Crystals, Van Nostrand, Princeton, 1968.
[8] N. Sagawa, H. lba, M. Urata, Y. Ozawa, J. Nucl. Sci. Technol. 13 (7) (1976) 358.
[9] W.F. Brehm, P.L. Koehmstedt, E.A. Kovacevich, D.W. Shannon, in: Joseph E. Darley, John R. Weeks (Eds.), Corrosion by Liquid Metals, Plenum Press, New York, London, 1970, p. 97.
[10] J. Ortega, M.A. Ariza, Liquid Metal Engineering and Technology, vol. 1, Oxford, UK, 1984, p. 523.
[11] A.I. Lastov, E.A. Pavlinchuk, E.E. Konovalov, Sov. At. Energy 60 (4) (1986) 308.
[12] V. Ganesan, P. Muralidaran, K. Chandran, G. Periaswami, in: Proc. Int. Symposium on Radiochemistry and Radiation Chemistry, Bhabha Atomic Research Centre, Bombay, 1991, p. SSC-37.1.
[13] J. Kremser, A. Lacroix, Proc. Int. Conf. on Liquid Metal Technology in Energy Production, CONF-760503, Champion, PA, 1976, p. 1.
[14] J.T. Holmes, C.R.F. Smith, W.H. Olson, Proc. Int. Conf. on Liquid Metal Technology in Energy Production, CONF-760503, Champion, PA, 1976, p. 12.
[15] H.H. Stamm, H.D. Hanke, H. Claus, Proc. Second Int. Conf. on Liquid Metal Technology in Energy Production, CONF-80040, Richland, Washington, 1980, p. 17.
[16] K. Nohara, K. Hirano, Proceeding ICSTIS, Suppl. Trans. ISIJ 11 (1971) 1267.
[17] A.F. Smith, R. Hales, Met. Sci. 9 (1975) 181.
[18] A.F. Smith, Z. Metallkd. 66 (11) (1976) 692.
[19] S. Paulinov, A.M. Gladyshev, V.N. Sugonyaev, lzv. Akad. NAUK, SSR, Met. 147 (1980) 5.
[20] K. Nohara, K. Hirano, J. Jpn. Inst. Met. 37 (1973) 51.
[21] R.P. Colburn, Specialists Meeting on Sodium Removal and Decontamination, Richland, IAEA Report IWGFR/23, 1978, p. 157.